J Mater Sci (2007) 42:8130–8138
DOI 10.1007/s10853-007-1728-1

In situ SALS and volume variation measurements during deformation of treated silica filled SBR

J. Ramier · L. Chazeau · C. Gauthier · L. Stelandre · L. Guy · E. Peuvrel-Disdier

Received: 5 September 2006 / Accepted: 26 March 2007 / Published online: 12 June 2007

Abstract Original in situ measurements of volume variation and small angle light scattering (SALS) are performed on silica filled Styrene Butadiene Rubber (SBR) during tensile tests. The influence of the silica treatment on the mechanisms involved is explored with sample carefully characterised and with the same filler dispersion. Two different types of silane are used as treatment, an alkoxy silane (so called covering agent) and a coupling agent which enables covalent bonds between the silica and the polymer matrix. It is shown that the coupling agent delays void formation in the samples and leads at intermediary strain to the reorganisation of the filler structure while the covering agent eases the void formation which also occurs without silica surface treatment.

Introduction

Though their large and growing industrial applications, the mechanical behaviour of silica filled elastomers, and more generally of nanoscopic filler/elastomer composites, is still the object of a vivid scientific debate concerning the mechanisms involved [1–4]. This is the case at small deformation, in the deformation range of the so-called Payne effect, as well as in the large deformation range. Indeed, due to the nanoscopic size of the silica, the large interfacial area combined to the small inter-filler distance leads to important filler–filler and filler matrix interactions whose consequences on the mechanical behaviour are still difficult to understand and model.

In particular, such interactions lead to the formation of a complex filler macrostructure within the polymer matrix, with mixed filler–filler and filler–matrix–filler junctions [5]. Moreover, they strongly influence the filler macrostructure evolution during deformation at large strain as well as the damage development at the interface. And, this has in turn strong involvements in the global mechanical response of the material. Indeed, the reinforcement level provided by the fillers is directly related to their organisation in the matrix and to the efficiency of the stress transfer through their interface [6, 7]. Moreover, the void formation implies a modification of the 3-dimensional response of the material.

Therefore, it is obvious that the mechanical behaviour at large strain of filled elastomer involves complex interrelated phenomena, whose each contribution to the material response is not clearly understood. It is the objective of the authors to address this question. To do so, different original experiments performed in situ during the sample deformations are presented. Volume variation measurements are performed to evaluate the void formation inside the materials as well as in situ SALS measurements to complete the characterisation of the void growth and characterise the microstructure evolution of the composites. Moreover, we used the possibilities given by different surface treatment of the silica particles. We have studied

J. Ramier · L. Chazeau (✉) · C. Gauthier
MATEIS (UMR CNRS 5510), INSA-Lyon, 69621 Villeurbanne Cedex, France
e-mail: laurent.chazeau@insa-lyon.fr

L. Stelandre · L. Guy
Rhodia Silices, 15 Rue Pierre Pays, B.P. 52, 69660 Collonges au Mont d'or, France

E. Peuvrel-Disdier
Ecole des Mines de Paris, Centre de Mise en Forme des Matériaux, 1, Rue Claude Daunesse, 06904 Sophia Antipolis Cedex, France

elastomer filled with silica particles untreated or treated with two different types of grafting agents: coupling agents which enable covalent bonds between the silica fillers and the styrene butadiene matrix, or covering agents which cover the silica surface with alkyl chains.

Materials and experiments

Materials

The elastomer is a SBR (Styrene Butadiene Rubber provided by Bayer S.A., Mn = 150,000 g/mol, Ip = 2) with 25 wt.% of styrene, 55 wt.% of 1–2 polybutadiène and 20 wt.% of 1–4 polybutadiene, without oil. The filler (Z1165 MP® from Rhodia) is a highly dispersible silica with a BET surface area of 160 m^2/g. The volume fraction introduced in the polymer is constant and equal to 50 phr (parts in weight per hundred parts of rubber). Considering the complete formulation (Table 1), it represents 20 vol.%. The curing system based on sulphur and vulcanisation activators and accelerators is introduced with the same amount for all the samples (Table 1).

The covering agent is triethoxy octyl silane. The coupling agent is the (bis(tri-ethoxysilylpropyl)-disulfane (TESPD), it is based on the same reactive foot (triethoxy) but with a reactive head that can establish covalent bonds between the matrix and the filler. Both covering (AR) or coupling (AC) agents were introduced in different concentrations. They can be either expressed in g/nm^2 of silica, taking 160 m^2/g as the specific surface of silica, or in number of feet/nm^2 of silica, knowing that there is one reactive triethoxy foot in a AR molecule, and two feet in a AC one (Table 2).

The samples are processed using a calander device (Banbury) following the Michelin patent RAULINE [8]. The first step is a shearing of the matrix and the incorporation of the fillers in the polymer with that of the antioxydant 6PPD (paraphenylene diamine). This shearing step lasts 5 min. First, the matrix is introduced in the internal mixer (Banburry with a 1l chamber and with tangential rotors, the filling is 90% of the chamber and the rotor speed 70 rpm) and sheared for a couple of minute and the organosilane molecules are introduced with 2/3 of the silica ratio; the rest is introduced after few minutes of shearing. After one night at ambient temperature, a second step enables the optimisation of the dispersion and of the grafting process initiated during the first step, as well as the incorporation of the ZnO. The third step is the incorporation of the vulcanisation system, i.e. sulphur, and the accelerators CBS (*n*-cyclohexyl-2-benzothiazyl-sulfenamide) and DPG (diphenylguanidine), performed on an open mill (two 160 mm diameter cylinders, the friction ratio is fixed at 1.2, i.e. the cylinders rotation speeds are 20 and 24 rpm, the gap is 3 mm) for 8 min, at low temperature (80 °C) to prevent any reaction of the vulcanisation system. After one night at ambient temperature, the last step is the vulcanisation in a press at 150 °C during 50 min (applied pressure of 150 bars). The samples obtained are 2 mm or 0.1 mm thick films.

Table 1 Formulation of the blends

BLEND	phr	Per hundred of matrix
Matrix	100	SBR 5525-0
Filler	50	Silica Z1165 MP
Surface treatment	Variable	Covering or coupling agent
S	1.1	Crosslinking system
CBS	1.3	Vulcanisation accelerators
DPG	1.45	
6PPD	1.45	Antioxidant
Acid stearic	1.1	Vulcanisation activators
ZnO	1.82	

Table 2 Sample name with their silane nature and content

Silica (phr)	Surface treatment	Concentration (phr)	Number of feet per nm^2 of silica	Concentration (10^{-23} g/nm^2 of silica)	Name
0	–	–		–	Matrix
50	–	–		–	MSi
50	AR	1.02	0.28	12.8	AR-3
50	AR	2.05	0.56	25.5	AR-6
50	AR	3.07	0.84	38.3	AR-8
50	AR	4.08	1.11	51	AR-11
50	AR	5.12	1.4	63.8	AR-14
50	AC	0.88	0.28	11	AC-3
50	AC	1.76	0.56	22	AC-6
50	AC	2.64	0.84	33	AC-8
50	AC	3.52	1.12	44	AC-11
50	AC	4.4	1.4	55	AC-14

AR is used for covering agent, AC for coupling agent

The characterisation of the grafting was performed by bound rubber measurement and water adsorption of the material [9]. The grafting occurred as expected from literature. The maximum coverage of the surface is obtained for around 4 phr of AR introduced, or around 3.5 phr of AC introduced. A higher quantity of grafting agents leads to a supplementary crosslinking within the matrix in the case of the coupling agent. Moreover, the use of the silane treatments limits the filler–matrix interactions, leading to a decrease of the bound rubber. The vulcanisation of the matrix is influenced by the silica treatment as shown by torque measurement during the sample curing [10]. This is

due to physical adsorption of the vulcanisation accelerators on the silica surface. This adsorption is decreased when silane are grafted on the surface. This should lead to a slightly more homogeneous crosslinking in the bulk matrix when the silica surface is covered. The filler dispersion was also carefully checked by Small angle scattering, and Transmission Electron microscopy (TEM) on cryomicrotomed sections, completed by observations (courtesy performed by F.E.I Corporation) with a Scanning Electron microscopy of surface prepared by Focused Ion Beam [11]. Figure 1 presents some of the results obtained. On the left, one can see that the pictures obtained for MSI, AR-8 and AC-8 samples do not show significant differences in the dispersion. Moreover, the scattering spectra obtained with the same samples with X-ray (D2AM line—ESRF Grenoble, France) and light sources (experiments performed at CEMEF) are similar. Thus, all the microstructural characterisations lead to the same conclusion: though the difference of surface treatments, the silica dispersion at the different observed scales is the same in all the tested samples.

Techniques

Small Angle Light scattering (SALS) has been performed with a laser source with a wavelength of $\lambda = 632$ nm. The scattering pattern is collected on a CCD camera. The momentum transfer q is defined as

$$q = \frac{4\pi}{\lambda}\sin\left(\frac{\theta}{2}\right) \tag{1}$$

where θ is the scattering angle. Its range spread from 9.6×10^{-5} to 4×10^{-4} Å^{-1}. The measurements have been performed at the CEMEF (Ecole des Mines de Paris, Sophia Antipolis). This technique needed the processing of sample with a 0.1 mm thickness to obtain a sufficient transmission of the intensity. The vulcanisation has been performed between Kapton films to avoid their deformation. These films enable a unmoulding without deterioration and protect the samples from pollution. These techniques have been performed during in situ tensile tests. Each acquisition is corrected by the thickness decrease during the sample stretching. This decrease has been estimated from the dilatational measurement with the formula:

$$e = e_0\left[\left(\frac{\Delta V}{V_0} + 1\right)\frac{L_0}{L}\right]^{0.5} \tag{2}$$

where e_0 is the initial thickness, L_0 the initial length, and L the length during stretching.

An angular average of the scattering pattern has been performed on an angle of 30° width in the parallel and the perpendicular directions.

Uniaxial tensile tests have been performed on a MTS machine 1/ME equipped with an extensometer. The samples are maintained during the stretching by pneumatic clamps to avoid their slipping. The samples are dumbbell shaped with a useful length of 20 mm, a 5 mm width and a 2 mm thickness. The crosshead speed is fixed at 500 mm/min and 3.6 mm/min corresponding to an initial strain rate of 0.4 and 0.003 s^{-1}, respectively. Tests have been performed at ambient temperature (25 °C).

Volume variation measurements were performed with a home-made apparatus designed from the principle of the Farris dilatometer [12, 13]. The volume variation is deduced from the measurement of the differential pressure between a reference chamber and the chamber containing the sample in an inert gas. A tensile test device is installed in this chamber to stretch the sample during the measurements. The precision of the apparatus is $\frac{\Delta Ve}{Ve} < 3 \times 10^{-3} = 0.3\%$ for an initial sample volume of 300 mm^3. It is much better than that of the old Farris system. This is partly thanks to: (i) a new generation of pressure sensors, (ii) a minimisation of the gas chamber, (iii) a complete temperature insulation of this chamber with two large volume envelops around. But the main innovation is a transmission of the tensile strain through the wall of the gas chamber by a rotating arm (then converted in traction with a drive-rack) and not by a transmission by translation, which always leads to gas leakage from the chamber. Note that this apparatus was also preferred to a videoextensometer owned by the laboratory

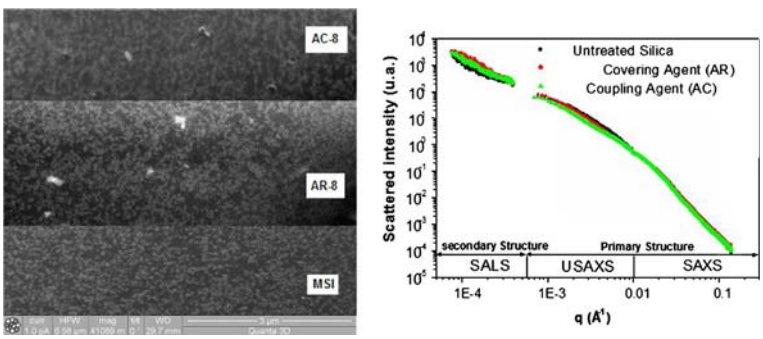

Fig. 1 Scanning Electron microscopy of surface prepared by Focused Ion Beam of MSi, AR-8 and AC-8 samples (left). Scattered intensity of the same samples as a function of the wave factor, obtained from SALS, USAXS and SAXS measurements (right)

(commercialised by Apollor) [14]. Indeed, the latter leads to much larger uncertainties in the volume variation measurement at large strain due to the deformation of the dots painted on the sample for the measurement, and to the fact that the measurements are deduced from local surface information.

The sample dimensions between the clamps were $15 \times 10 \times 2$ mm^3. Due to the machine limitations, in the case of the samples studied here, note that the maximum deformation is 300%, with a maximum strain rate of 0.003 s^{-1}. Force, temperature, displacement are also collected during the test.

Results and discussion

Figure 2a presents the nominal stress–strain curve of the SBR matrix and the silica filled SBR composite obtained with a tensile test. The use of silica increases the stress measured at a given deformation and increases both stress and strain at break (from 5 up to 7.5 for the strain and from 4 to 18 MPa for the stress).

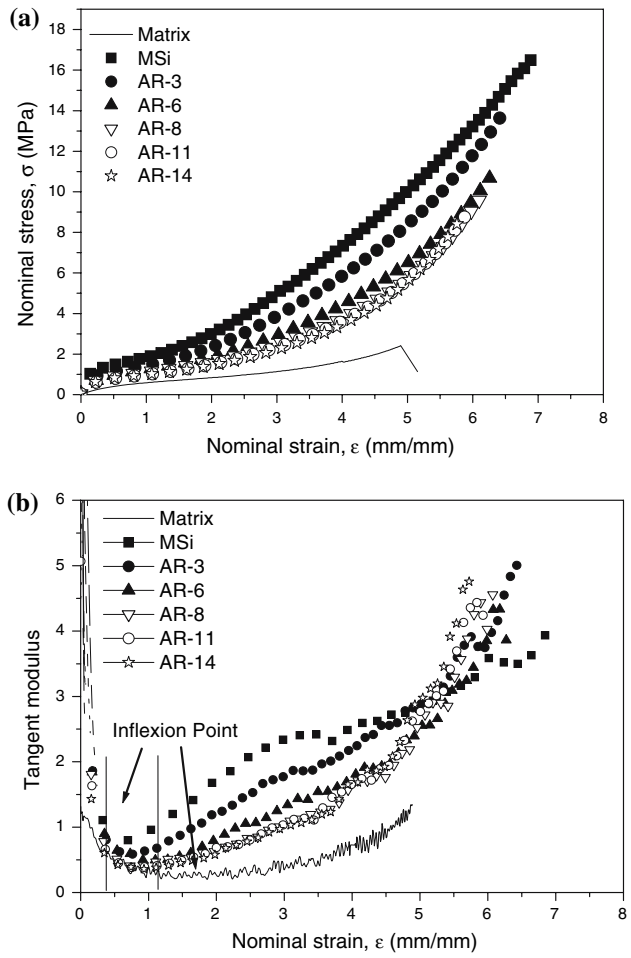

Fig. 2 Tensile test performed at ambient temperature with $d\varepsilon/dt = 0.4$ s^{-1} on the AR series. (**a**) Nominal stress–strain curve, (**b**) tangent modulus as a function of the nominal strain

To interpret the reinforcement at large deformations, one can consider the role of the strain amplification due to the fillers. Indeed due to heterogeneities in the filler distribution, zones of lower modulus deform more than more rigid ones [15, 16]. Locally, the strain becomes higher than the macroscopic one [17]. Following Kucherskii [18], the amplification factor can be estimated from the strain level at the minimum of the tangent modulus. This point corresponds to the inflexion point on Fig. 2b. Following this author, the position of this point is significant of the extension limit of the shorter polymer chains in the vulcanised network. An amplification factor can be defined as:

$$K = \varepsilon_{\text{kmatrice}} / \varepsilon_{\text{kcomposite}} \tag{3}$$

where $\varepsilon_{\text{k matrice}}$ and $\varepsilon_{\text{k composite}}$ are the macroscopic deformation of the pure gum and of the composite, respectively. A value of 2.8 for the silica filled SBR (MSi sample) is found.

Figure 2 also presents the tensile test stress–strain curves of the AR series. The increase of the AR content leads to a decrease of the stress at a given strain level. This decrease of the stress is stabilised for an AR content above 3 phr. It can be due to a progressive covering of the silica surface. This in turn decreases the rigidity of the filler structure by decreasing the quantity of bound rubber transmitting the stress between the filler sub-structures that are less deformed. The AR content at which the phenomenon stabilises corresponds to the total covering of this surface. Concerning the tangent modulus plotted on Fig. 2b, the curves can be separated in three regions, respectively, between a strain of 0 and 1, 1 and 5 and above 5. In the first region, (ε between 0 and 1), the initial modulus value decreases progressively when the AR content increases. An increase of the AR content increases the strain at the minimum of the tangent modulus and decreases the value of this minimum from 0.8 down to 0.3 MPa. Consequently, as shown on Fig. 3, the amplification factor slightly decreases as a function of the AR content down to a threshold value of 2.2. This suggests that the use of a covering agent leads to a narrower distribution of the chain length between crosslinks. This confirms the results of Ref. [9] where it is shown that the use of AR decreases the adsorption of the CBS and consequently leads to a more homogeneous vulcanisation, less localised in the filler neighbourhood.

In the second region (ε between 1 and 5), the tangent modulus decreases with the AR content. An inflexion of the curve is visible for strain close to 3 for the samples MSi and AR-3 and is followed by a plateau. This is not observed for the other samples. Our assumption is that in the other

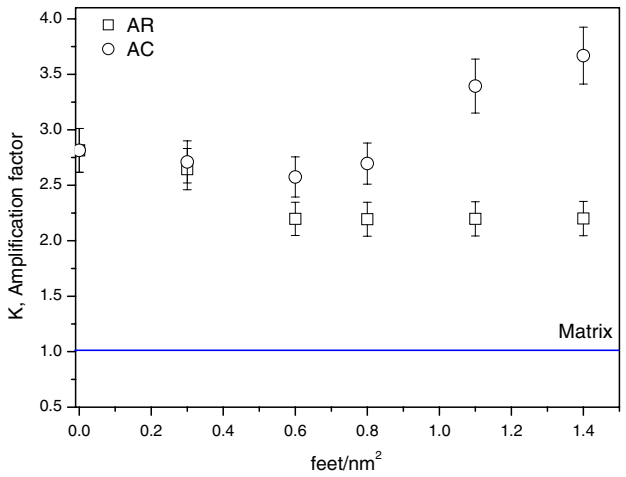

Fig. 3 Amplification factor as a function of AR and AC content

samples of the AR series, at these strain levels, the first break of the filler network and the desorption of the bound rubber linking the sub-structures already occurred and the first decohesions appear. These decohesion are made easier when the filler–matrix interactions are weak; this leads to tangent moduli which increase more progressively after the first inflexion point.

In the third region ($\varepsilon > 5$), the order of the curves is inverted, and the moduli are lower for MSi and increases with the AR content. In this strain hardening zone, all the network chains reach their limit of extensibility. The properties are therefore mainly controlled by the average state of crosslinking. As recalled previously, the more the silica surface covered by AR, the less adsorbed the CBS accelerator, and therefore the shorter and more numerous the sulfur bonds. This terminal zone would reflect this phenomenon by a more rapid hardening and a slightly smaller strain at break, as shown on Fig. 2. However, the strain at break lies in a narrow range (between 5.7 and 7) when the range of stress at break is large (between 8 and 16 MPa). Following our previous assumption, the sample deformation is concentrated in the matrix ligaments created between the zone where the decohesion occurred. Therefore the effective sample section which resists to the deformation decreases when the decohesion is important. However, the strain at break of these ligaments is not modified (if the slight difference of crosslinking discussed above is neglected). This explains a constant strain at break and a decreasing stress at break with the increasing AR content.

Figure 4 presents the tensile stress–strain curves for the AC series. At a given strain, the stress level increases when the coupling agent ratio increases. The strain at break decreases with increasing silane content, from 7 for the untreated silica down to 3 for the AC-14 sample. The

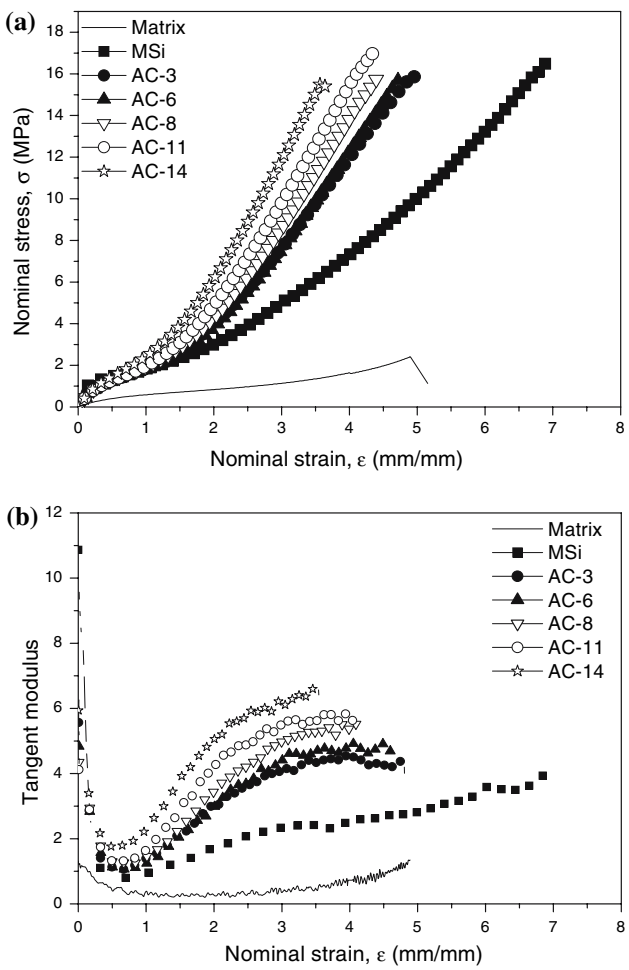

Fig. 4 Tensile test performed at ambient temperature with $d\varepsilon/dt = 0.4\ s^{-1}$ on the AC series. (**a**) Nominal stress–strain curve, (**b**) tangent modulus as a function of the nominal strain

nominal stresses at break are in a narrow range, which means that the true stress at break increases with increasing AC content. Tangent moduli as function of the strain are plotted on Fig. 4. The deduced amplification factor is plotted on Fig. 3. It slightly decreases for AC content up to 3 phr and slightly increases for higher silane content. As described in Ref. [9], at these levels of AC content, the grafting of the surface is maximum. The evolution of the amplification factor can be the result of two phenomena, the covering of the surface which leads to a more homogeneous crosslinking and the increase of the crosslinking density due either to the supplementary covalent bonds between the filler and the matrix, or to the excess of AC which has polycondensed. However, it is noteworthy that the decrease of the amplification factor observed for AC ratio up to 3 phr is the same as that observed with AR. This means that the crosslinking heterogeneities introduced by the covalent bonds at the filler surface are not at the origin of the hardening in its early phase. One can also notice that

the minimum of the tangent modulus increases with the AC content, from 0.8 to 1.7 MPa. This is the signature of the increasing crosslink number. As shown on Fig. 4b, for higher strain level, the tangent modulus increases with the AC content and reaches a plateau whose value obviously depends on the global crosslinks density (i.e. including the filler–matrix covalent bonds).

Thus, the silica increases largely the mechanical properties of the SBR. When it is treated by covering agent, this effect tends to decrease. Conversely the use of a coupling agent leads to a more important reinforcement due to the formation of supplementary covalent bonds, but to a decrease of the strain at break. In this range of deformation, the nature of the interface, more resistant with coupling agents or weaker with covering agents, is a determining factor. The influence of AC on the stress and strain at break is very different from that of AR. The use of a coupling agent, conversely to that of the covering agent, would limit the decohesion between the matrix and the silica. This phenomenon would be either delayed or replaced by another type of damage. In the case of coupling agent, indeed, some authors consider the formation of cavities in the matrix [19]. Whatever the damage mechanism, the decrease of the slope of the tangent modulus curve is interpreted as a result of this damage. The following measurements are devoted to its characterisation by volume variation measurement or small angle light scattering.

Volume variations under tensile test of the AR series are reported on Fig. 5. Note that it has been checked that the matrix does not present any volume variation when tested. This results confirms the quasi incompressibility of the unfilled elastomer (Poisson coefficient of 0.4999) and validates the technique. With fillers, the volume variation begins at the beginning of the tensile test and increases with strain up to a value of 4% for a nominal strain of 3. As shown on Fig. 5, the use of a covering agent does not modify this trend. But at a given strain, the volume variation decreases with the AR content. Plotted as a function of the stress, the contrary is observed, i.e. an increase of the volume variation as function of the stress with the AR content. The stress necessary to obtain the beginning of the volume variation is lower, whatever the silica treatment.

Figure 6 presents the volume variation under tensile test as a function of the nominal strain for the AC series. One can observe that the concavity of the curves is different from that of the AR series curves. The volume variation occurs for deformation around 0.5 when it occurred at the beginning of the deformation for the AR series. Besides, this volume variation increases with strain to pass over that observed with the AR series. The volume variation plotted as a function of the stress on Fig. 8b show superimposable curves whatever the AC ratio. About 1 phr of coupling agent seems enough to modify the volume variation

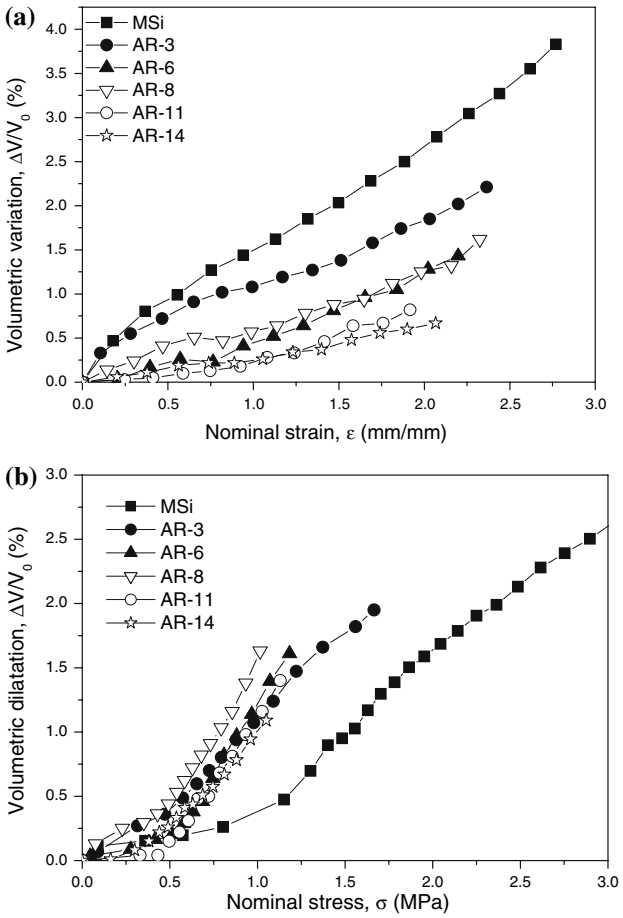

Fig. 5 Volume variation for the AR series, during tensile test, as a function of (**a**) nominal strain and (**b**) nominal stress

mechanism. These curves show the absence of cavitation for stress below 1 MPa. Thus, the coupling agent delays the occurrence of decohesion at low strain.

To confirm these results, small angle scattering during tensile tests has been performed. SAXS and USAXS did not show any variation of the scattering pattern during the deformation conversely to SALS whose results are presented below. The study was limited to the matrix, MSi, AC-8, AC-14 and AR-8. Like in volume variation measurements, the difference lies in the presence or not of covalent bonds between the filler and the matrix. For this reason, we will only present the results obtained with AC and MSi. As presented in Ref. [11], the initial scattering pattern is isotropic whatever the silica surface treatment. This scattering is the signature of the large silica agglomerates. The scattering was measured continuously with deformation. From these measurements, two significant domains have been distinguished, the first is at nominal strain below 100%, the second above. In each of these domains, we have selected two strains for which the scattering pattern is representative:

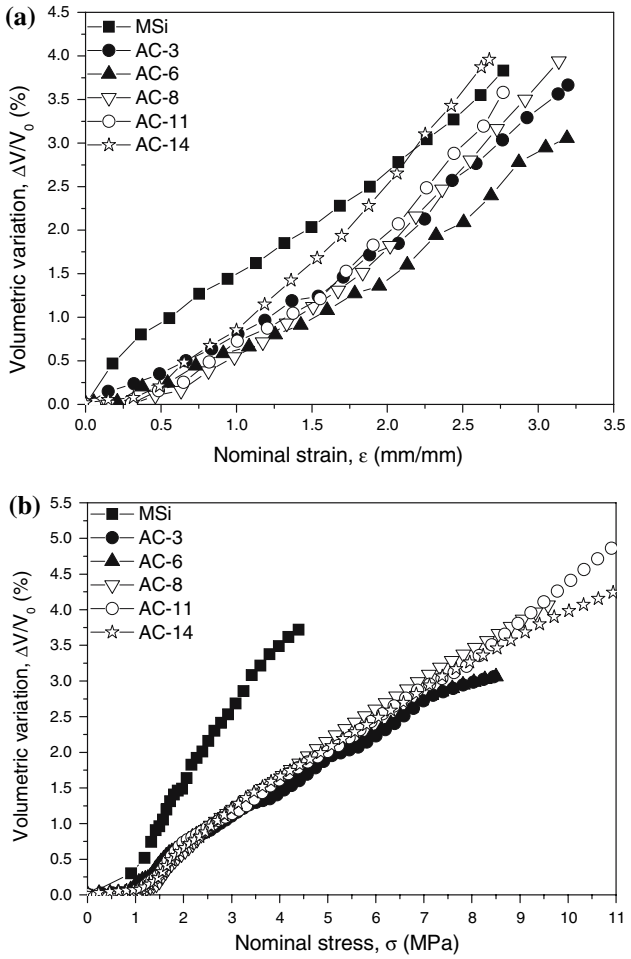

Fig. 6 Volume variation for the AC series, during tensile test, as a function of (**a**) nominal strain and (**b**) nominal stress

– At nominal strain of 75%. At this level, volume variation showed a big difference between sample with and without coupling agents, while the stress is the same for both samples.
– At nominal strain of 250%, when the stress levels are very different and the volume variation values are close.

Profiles obtained at 75% are presented on Fig. 7. Note that the matrix did not show any evolution of its scattering pattern. The latter includes the scattering of ZnO. But its small concentration leads to a distance between ZnO particles too large to be visible with this technique, even more when the sample is stretched. Moreover, the absence of any modification of the matrix profile also showed that the ZnO agglomerate are not affected by the deformation. This means that any modification of the scattering pattern in the silica filled samples cannot be ascribed to the matrix and its ZnO content.

The stretching of MSi leads to a scattering pattern stretched perpendicularly to the tensile direction. This

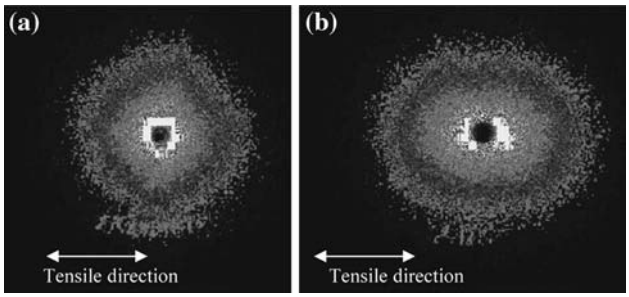

Fig. 7 Scattering patterns at 75% nominal strain of (**a**) Msi and (**b**) AC-8

pattern corresponds to the scattering of entities stretched in the tensile test direction. The volume variation measured at this strain level enables to associate this scattering to the presence of voids. With coupling agents, the scattering pattern observed is different. As confirmed by volume variation measurement, this pattern cannot be the signature of voids. The formation of a so-called ''butterfly'' pattern has also been reported in literature. Bastide et al. [20] observed it in the case of swollen gel, in which heterogeneities of crosslink density leads to deformation heterogeneities during tensile test. Besides, DeGroot et al. [21] observe this phenomenon for colloidal silica suspension in PDMS (polydimethylsiloxane) under shear. They claimed that the scattering observed is the result of the rupture and the reorganisation of silica agglomerates by their contraction and orientation in the tensile direction. Our results correspond to this case. The coupling agents, by limiting the decohesion at the interface, enable a stretching of the filler sub-structures made of several filler aggregates. This stretching necessarily heterogeneous leads to the occurrence of new correlation lengths in the stretching direction.

Figure 8 presents the scattering patterns obtained at 250% strain. In the case of MSi, the trend already observed at 75% is amplified. The scattering entities (voids) lengthened. For the coupling agent treated silica, the scattering pattern has a profile perpendicular to that observed at 75%, similar to that of MSi. The visualisation of all the intermediary patterns shows that it is the result of a progressive

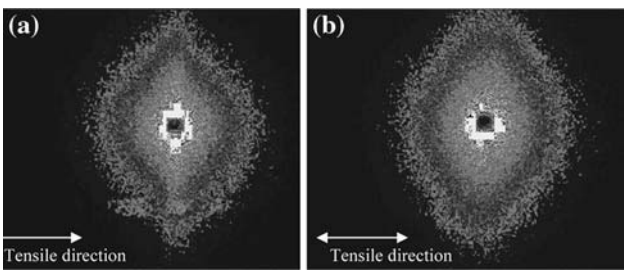

Fig. 8 Scattering patterns at 250% nominal strain of (**a**) MSi and (**b**) AC-8

increase of its width in the direction perpendicular to the tensile direction when that in the parallel direction slightly decreases. The scattering of stretched entities is added to the scattering due to the filler reorganisation. The volume variation measurements show that, like for MSi, these entities are voids.

The intensity as a function of Q in both parallel and perpendicular direction to the tensile direction has been deduced from the scattering pattern following the procedure described in the experimental section. The example of MSi is shown on Fig. 9 in the perpendicular direction to tensile direction. At strain equal to zero, the intensity plotted in logarithmic scale shows a maximum slope of –1 characteristic of a very open fractal mass. The application of a strain does not change the global shape of the pattern but leads to a global increase of the intensity which is due to the increase of the number of scattering entities. None characteristic length is visible. Therefore, the classic Guinier treatment cannot be applied to determine their size. This is apparently due to the too large distribution of their size. Note that the presence of badly dispersed ZnO in the matrix made unfortunately impossible the subtraction of the matrix signal to the intensity obtained and therefore impossible a more quantitative treatment than the following.

Debye et al. [22] show that the intensity scattered by an isotropic biphasic structure, writes:

$$I(q) = C\int_0^\infty r^2\gamma(r)\frac{\sin(qr)}{qr}dr \tag{4}$$

where $\gamma(r)$ is the correlation function representing the distance distribution between regions of different refraction index. If the distribution is random, the correlation function writes:

$$\gamma(r) = \exp(-r/a_1) \tag{5}$$

where a_1 is the average correlation distance. The intensity can be simplified by combining both equations:

$$I(q) = Cte + \frac{w}{(1 + q^2a_1^2)^2} \tag{6}$$

where Cte is a constant and w is proportional to a_1^3.

This expression simulates correctly the intensity curves as shown on Fig. 9. The found correlation lengths (parallel and perpendicular) are plotted on Fig. 10 as a function of the strain. The evolution of the correlation length perpendicularly to the tensile test direction is similar for both samples. This length can be associated to the lateral dimension of the stretched voids in the tensile direction. The slight difference between both samples at low strain can be explained by the delay of the void formation in the case of the AC-8 samples. In the parallel direction, the

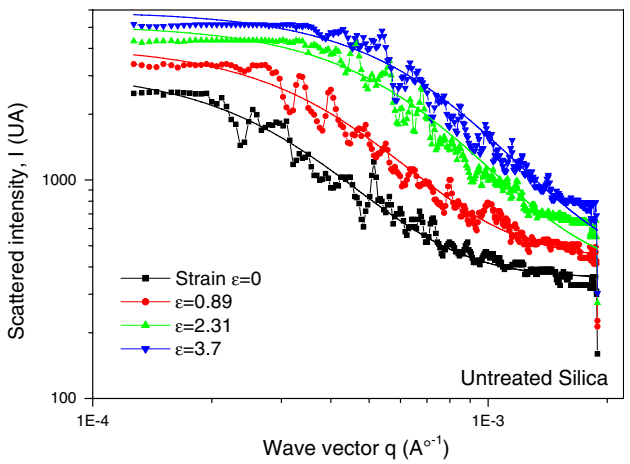

Fig. 9 Scattering profile of MSi in the perpendicular direction to the stretching direction at different strain level

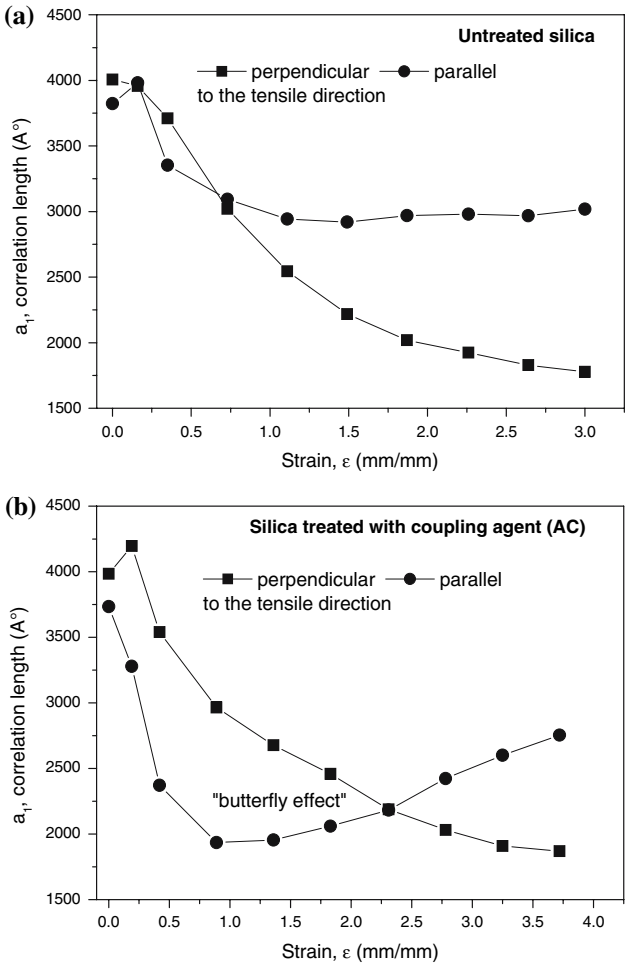

Fig. 10 Correlation length deduced from the scattering patterns as a function of nominal strain for (**a**) MSi and (**b**) AC-8 sample

behaviour of the different samples is different. The correlation length decreases for both samples up to a strain of 0.75. The drop is more important for the AC sample. Then, for this sample, the correlation length increases when it is almost constant for MSi. Note that the values tend to join at large deformation. The difference noticed corresponds to the appearance of the butterfly pattern described above. These results also show that the cavitation process is very similar for both samples at large deformation, as previously suggested by the simple observation of the scattering patterns. The stability of the correlation length in the case of the MSi can seem paradoxical if one assumes that it is only associated to the length of the stretched voids in the tensile direction (one expected an increase of this length with strain). This suggests that the volume increase is done by nucleation of cavities more and more numerous instead of growth of voids created at the beginning of the test.

Conclusion

The mechanisms involved in the deformation of silica filled elastomers are complex interrelated phenomena dependent on the filler surface chemistry. To evidence it, we have prepared samples with filler modified with either coupling agents or covering agents, and in which the filler dispersion is the same. These samples have been tested with an original combination of dilatometry and SALS performed in situ during tensile tests. In all samples, the mechanisms involved are firstly a weakening of the mixed polymer filler network at the level of the filler sub-structure junctions in this network, then a deformation of the vulcanised network and damage. Our results evidence two tendencies as a function of the surface treatment:

- when using a covering agent, the reinforcement decreases with the surface covering. This decrease is due to the lower quantity of bound rubber involved in the stress transfer between the sub-structures during deformation. Moreover, the use of these covering agents eases the decohesion and the void formation which are going to limit the stress transfer. This leads to high strain at break and a decreasing stress at break.
- when using a coupling agent, one observes an increasing reinforcement with the AC content, silica fillers then become multifunctional crosslinking nodes which considerably increase the crosslinking effect. The strong cohesion at the interface maintains the stress transfer and delays the occurrence of decohesion. This delay allows a reorganisation of the sub-structure. However, when the damage is initiated, voids grow more rapidly with the deformation due to the higher stress level. Moreover, the increase of the global crosslink density leads to a decrease of the average length between crosslinks and therefore to a decrease of the strain at break.

To conclude, the modification of the filler interface, with same filler dispersion, drastically changes the mechanical behaviour. The hardening part of the stress–strain curves is the result of concomitant mechanisms such as decohesion, void formation and heterogeneous evolution of the filler microstructure. Therefore, to the authors' opinion, the development of a micromechanical approaches for the description of the mechanical behaviour of filled elastomer will be only meaningful if they account for the interface strength as well as the creation of the supplementary phase of void created by the interface damage.

Acknowledgements The authors are indebted to C. Rochas for preliminary SALS experiments performed at ESRF, and to Drs. M.N. Bouchereau for fruitful discussions. This work was financed by Rhodia S.A.

References

1. Göritz D, Duschl E (1993) J Polymer 34(6):1216
2. Zhu A, Sternstein SS (2003) Comp Sci Technol 63(8):1113
3. Berriot J, Lequeux F, Monnerie L, Montes H, Long D, Sotta P (2002) J Non-Cryst Solids 307–310:719
4. Heinrich G, Klüppel M, Vilgis TA (2002) Curr Opin Solid State Mat Sci 6(3):195
5. Leblanc JL (2002) Prog Polym Sci 27(4):627
6. Lopez-Pamies O, Ponte Castañeda P (2004) Math Mech Solids 9(3):243
7. Diani J, Brieu M, Gilormini P (2006) Int J Solids Struct 43(10):3044
8. Rauline R (1992) Eur. Pat. 0 501227A1, to Cie. Generale de Etablissements Michelin-Michelin & Cie
9. Ramier J, Chazeau L, Gauthier C, Guy L, Bouchereau MN (2004) J Polym Sci Part B Polym Phys 2005, 44, 143; see also J. Ramier Ph-D Thesis, INSA-Lyon, 2004 at http://csidoc.insa-lyon.fr/these/2004/ramier/
10. Ramier J, Chazeau L, Gauthier C, Guy L, Bouchereau MN (2007) Rubber Chem Technol 80(1):183
11. Ramier J, Gauthier C, Chazeau L, Stelandre L, Guy L (2007) J Polym Sci Polym Part B Polym Phys 45:286
12. Farris RJ (1964) J Appl Polym Sci 8:25
13. Reichert WF, Hopfenmüller MK, Göritz D (1987) J Mater Sci 22:3470. DOI: 10.1007/BF01161444
14. G'sell C, Hiver JM (2002) Int J Solids Struct 39:3857
15. Mullins L, Tobin NR (1965) J Appl Polym Sci 9:2993
16. Lapra A, Bokobza L (2000) J Polym Sci: Polym Phys 38:2449
17. Westermann S, Pyckhout Jintzen W, Richter D, Straube E, Egelhauf S, May R (2001) Macromolecules 34:2186
18. Kucherskii AM (2003) Polymer Test 22(5):503
19. Nicholson DW (1979) J Adhesion 10:255
20. Bastide J, Leibler L, Prost J (1990) Macromolecules 23:1821
21. Degroot JV, Macosko CW, Kume T, Hashimoto T (1994) J Colloid Interf Sci 166:404
22. Debye P, Anderson HR, Brumberger H (1957) J Appl Phys 28:679